Supplemental information

Real-time visualization of carbon quantum dots transport in homogeneous and heterogeneous porous media

Ying Zhao[a,b,1], Jian Song[a,b,1], Qingchun Yang[c], Yuelei Li[d], Zhuqing Liu[a,b*], Fan Yang[a,b*]

a. School of Water Conservancy & Civil Engineering, Northeast Agricultural University, Harbin 150030, China

b. International Cooperation Joint Laboratory of Health in Cold Region Black Soil Habitat of the Ministry of Education, Harbin 150030, China.

c. Key Laboratory of Groundwater Resources and Environment Ministry of Education, Jilin University, Changchun 130021, China

d. School of Environment, Harbin Institute of Technology, Harbin, 150090, China

1 Ying Zhao and Jian Song contribute equally to this work and should be considered co-first authors.

* Corresponding Author: yangfan_neau@163.com

S1 The measurement of the ζ-potentials of quartz sand

For the measurement of the zeta potential of quartz sand we refer to the method of (Dong et al., 2016) and (Zhao et al., 2023)[1, 2]: Weigh 5.0 g of quartz sand and grind it in an onyx mortar, pass it through a 100 mesh sieve, transfer the sieved quartz sand powder into a beaker containing deionized water. Then ultrasonically disperse it for 30

min under the condition of 100 W, 45 kHz, and then suck up the upper layer of the suspension by siphoning. And then determine its zeta potential by Nano ZS90. At least 3 replicates were prepared for each sample, and each sample was measured at least 3 times during the measurement.

S2 CQDs TEM measure

The CQDs solution (100 $mg \cdot mL^{-1}$) was dropped on a carbon-supported copper mess (20 μL) and dried under infrared light. Then, transmission electron microscope (TEM) images were obtained using a JEM-2100 electron microscope (JEOL, Tokyo, Japan) with an accelerating voltage of 200 kV. The TEM characterization of other carbon nanomaterials is the same as that of CQDs.

S3 CQDs FT-IR measure

The KBr pressing method was used, and the samples and KBr were dried at 105 °C for 8 h prior to the test, and a small amount of the dried samples was taken to grind and mix the samples with KBr powder at a ratio of 1:100 (wt/wt). All FTIR spectra were collected in the mid-infrared range from 400 cm^{-1} ~ 4000 cm^{-1} with a step size of 4 cm^{-1} and a scanning rate of 40 cm^{-1}. In order to obtain clear peaks, it was necessary to mix the sample material and KBr completely.

S4 DLVO theory

Adoption of classic DLVO theory to calculate the interaction energy between particles during convergence. The stability of nanoparticles in stability in water depends on the vander Waals interaction energy (VDW) and the electrostatic double layer (EDL) energy [3].

$$\phi_{EDL} = \pi\varepsilon_0\varepsilon_r\alpha_r\left\{2\psi_s\psi_{bc}\ln\left[\frac{1+\exp(-\kappa h)}{1-\exp(-\kappa h)}\right]+\left(\psi_s^{\,2}+\psi_{bc}^{\,2}\right)\ln\left[1-\exp(-2\kappa h)\right]\right. \quad (1)$$

where ε_0 denotes the dielectric constant under vacuum, 8.845×10^{-12}C/(Vm); ε_r denotes the relative capacitance of water, 78.55 at 25℃; α_r denotes the average radius of colloid; h denotes the distance between the colloid and the medium; ψ_s, ψ_{bc} denotes the potential of the quartz sand and the CQDs, commonly used as ζ-potential is expressed; κ denotes the inverse of the debyehukel length denotes the reciprocal length of the debye-huckel reciprocal length (debye-huckel reciprocal length) and the expression is as follows:

$$\kappa = \sqrt{\frac{2\times10^3 e^2 N_A I}{\varepsilon_0\varepsilon_r kT}} \quad (2)$$

where k denotes the Boltzmann constant. 1.38×10^{-23} J/K; T denotes the absolute temperature; N_A denotes the Avogadro Rowe's constant. 6.022×10^{23}; e denotes the charge of the electron. 1.6×10^{-19}; I is the ionic strength.

$$\phi_{VDW} = -\frac{A\alpha_r}{6h}\left(1+\frac{14h}{\lambda}\right)^{-1} \quad (3)$$

which A is Hamaker constant; λ is the the characteristic wavelength (100nm). Finally, the total interaction energy is as follows:

$$\phi_{TOT} = \phi_{EDL} + \phi_{VDW} \quad (4)$$

S5 Calculation of theoretical model parameters for colloidal filtration

The single collector contact efficiency (η_0) is estimated by empirical equations[4], and is obtained by superimposing the contact efficiencies of the three sub-processes (single-collector contact efficiency for transport by diffusion (η_D), single-collector

contact efficiency for transport by interception (η_I) and single-collector contact efficiency for transport by gravitational sedimentation (η_G)), attachment efficiency (α) is the ratio of the number of colloids adsorbed by the collector due to collisions to the total number of colloids that collided in the collector ($0 \leqslant \alpha \leqslant 1$), the corresponding formulas are as follows:

$$\eta_0 = \eta_D + \eta_I + \eta_G \tag{1}$$

$$\eta_D = 2.4 A_S^{1/3} N_R^{-0.081} N_{Pe}^{-0.715} N_{vdw}^{0.052} \tag{2}$$

$$\eta_I = 0.55 A_S N_R^{1.675} N_A^{0.125} \tag{3}$$

$$\eta_G = 0.22 N_R^{-0.24} N_G^{1.11} N_{vdw}^{0.053} \tag{4}$$

$$\alpha = -\frac{2}{3}\frac{d_c}{(1-\theta)L\eta_0} Ln(\frac{C}{C_0}) \tag{5}$$

$$k_d = \frac{3}{2}\frac{(1-\theta)}{d_c\theta} U\alpha\eta_0 \tag{6}$$

N_R is the ratio of colloidal particle size to the particle size of the medium. N_{Pe} is the ratio of convective to diffusive transport of colloidal particles. N_{vdw} is the ratio of the van der Waals induced potential energy between the colloidal particles-medium particles to the particles' own thermal energy. N_A is the effect of van der Waals gravity between colloidal particles and flow velocity on the process of retention deposition of colloidal particles occurring on the surface of medium particles. N_G is the ratio of the Stokes settling rate of colloidal particles to the seepage flow rate, and sedimentation rate coefficient (k_d). The results of the parameters for different conditions are shown in Table S1.

Table S1.Summary of the η_0, η_D, η_I η_G and α for All the Experiments

No.	Particle size (μm)	IS（mM）	pH	θ	η_D	η_I	η_G	η_0	α	k_d
A1	**120-180**	1	7	0.30	0.1081	0.00032392	0.000046034	0.1085	7.93E-5	0.06026958
A2	**180-380**	1	7	0.32	0.0694	0.00009888	0.000053473	0.0696	2.23E-4	0.056772193
A3	**380-830**	1	7	0.37	0.0088	0.00000041	0.000111799	0.0089	3.72E-2	0.052296595
B1	180-380	**1**	7	0.32	0.0694	0.00009888	0.000053473	0.0696	2.23E-4	0.056772193
B2	180-380	**100**	7	0.32	0.0221	0.00076722	0.000921510	0.0238	7.29E-4	0.063271649
B3	180-380	**200**	7	0.32	0.0201	0.00090301	0.001155667	0.0225	8.30E-4	0.067327287
C1	180-380	1	**5**	0.32	0.0566	0.00014242	0.000088779	0.0569	3.02E-4	0.06260496
C2	180-380	1	**7**	0.32	0.0694	0.00009888	0.000053473	0.0696	2.23E-4	0.056772193
C3	180-380	1	**9**	0.32	0.1005	0.00005102	0.000021323	0.1006	1.49E-4	0.05480413

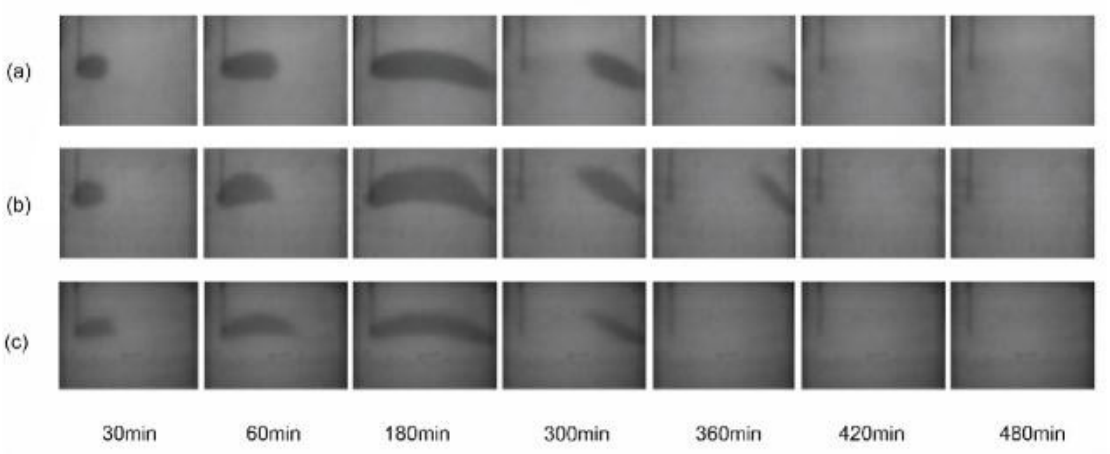

Figure S1. Original gray level images (a: coarse sand; b: medium sand; c: fine sand) of CQDs transport in 2-D homogeneous porous media under pH=7, IS=1mM.

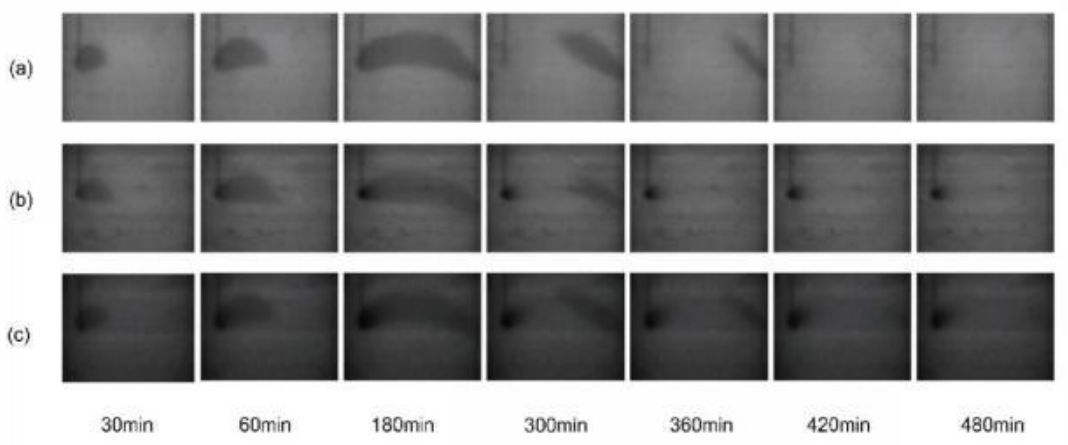

Figure S2. Original gray level images (a: at 1 mM; b: at 100 mM; c: at 200 mM) of CQDs transport in 2-D heterogeneous porous media under medium sand, pH=7.

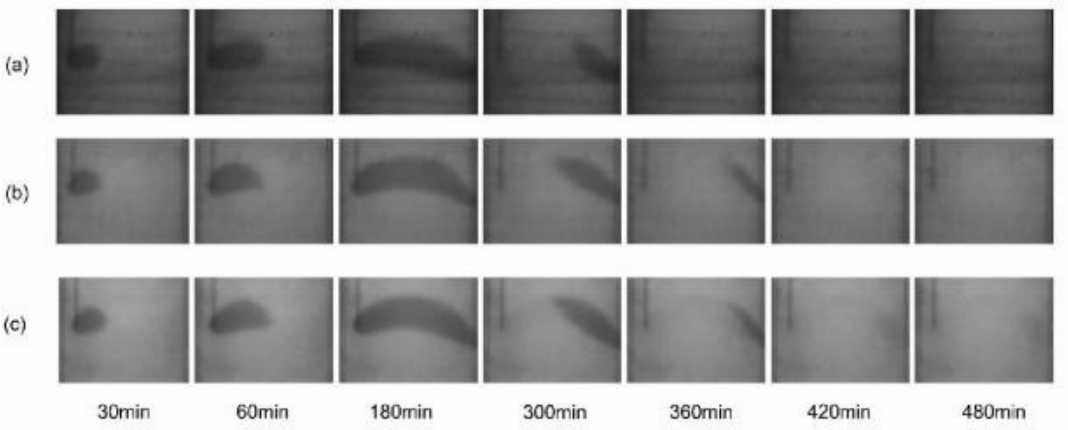

Figure S3. Original gray level images (a: at pH=5; b: at pH=7; c: at pH=9) of CQDs transport in 2-D heterogeneous porous media under medium sand, IS=1mM.

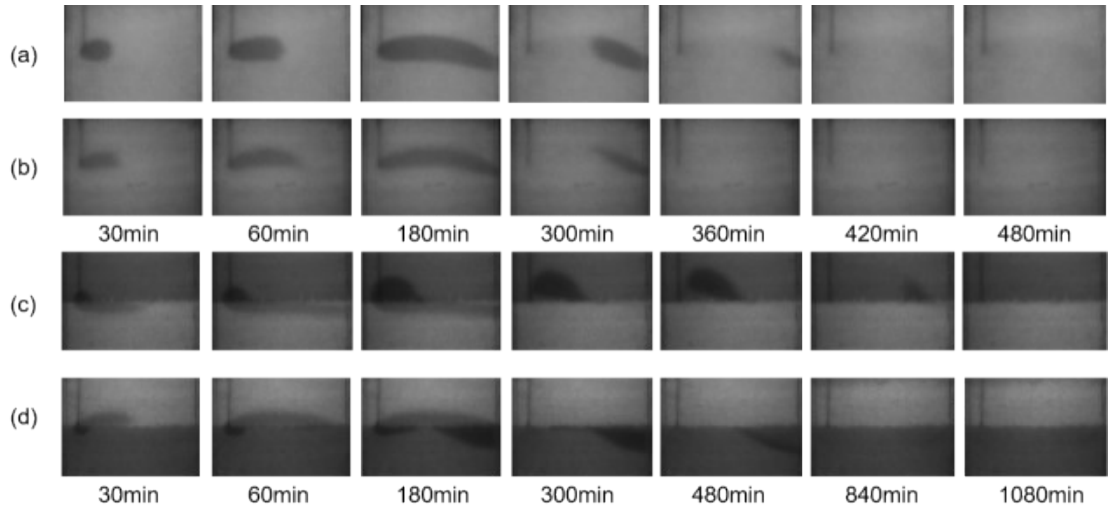

Figure S4. Original gray level images (a: homogeneous fine sand, b: homogeneous coarse sand, c: upper fine sand and lower coarse sand, d: upper coarse sand and lower fine sand) of CQDs transport in 2-D heterogeneous porous media under pH=7, IS=1mM.

1. Y. Zhao, D. Fan, S. Cao, W. Lu and F. Yang, *Journal of Hydrology*, 2023, **619**.
2. S. Dong, B. Gao, Y. Sun, H. Guo, J. Wu, S. Cao and J. Wu, *Journal of Hazardous materials*, 2019, **369**, 334-341.
3. Y. Zhang, Y. S. Chen, P. Westerhoff, K. Hristovski and J. C. Crittenden, *Water Research*, 2008, **42**, 2204-2212.
4. N. Tufenkji and M. Elimelech, *Environmental Science & Technology*, 2004, **38**, 529-536.